Mutations in the human *Jagged1* gene are responsible for Alagille syndrome

Takaya Oda[1], Abdel G. Elkahloun[2,5], Brian L. Pike[1], Kazuki Okajima[3], Ian D. Krantz[4], Anna Genin[4], David A. Piccoli[4], Paul S. Meltzer[2], Nancy B. Spinner[4], Francis S. Collins[1] & Settara C. Chandrasekharappa[1]

Alagille syndrome (AGS) is an autosomal-dominant disorder characterized by intrahepatic cholestasis and abnormalities of heart, eye and vertebrae, as well as a characteristic facial appearance. Identification of rare AGS patients with cytogenetic deletions has allowed mapping of the gene to 20p12. We have generated a cloned contig of the critical region and used fluorescent *in situ* hybridization on cells from patients with submicroscopic deletions to narrow the candidate region to only 250 kb. Within this region we identified *JAG1*, the human homologue of rat *Jagged1*, which encodes a ligand for the Notch receptor. Cell-cell Jagged/Notch interactions are known to be critical for determination of cell fates in early development, making this an attractive candidate gene for a developmental disorder in humans. Determining the complete exon–intron structure of *JAG1* allowed detailed mutational analysis of DNA samples from non-deletion AGS patients, revealing three frame-shift mutations, two splice donor mutations and one mutation abolishing RNA expression from the altered allele. We conclude that AGS is caused by haploinsufficiency of *JAG1*.

Alagille syndrome (AGS, MIM 118450) is an autosomal dominant disorder characterized by neonatal jaundice and a paucity of intrahepatic bile ducts on liver histology. Other accompanying features of this syndrome are congenital heart defects, especially pulmonic valvular stenosis and peripheral pulmonary arterial stenosis; abnormal 'butterfly' vertebrae and decreased interpediculate distance in the lumbar spine; posterior embryotoxon of the eye; and a typical facies consisting of a broad forehead, pointed mandible, deep-set eyes and a bulbous tip of the nose[1,2]. Variable degrees of learning disability and mental retardation have been reported, but most patients are of normal intelligence. The disease occurs at a frequency of about 1:70,000 births and is the second most common cause of intrahepatic cholestasis in infancy[3]. The expression of AGS can vary from an apparently normal phenotype to severe cases where liver failure requires liver transplantation.

Dhorne-Pollet *et al.*[4] examined 33 families ascertained through 43 probands and concluded that penetrance is 94% and that 15% of cases are sporadic. Other studies[5] have documented frequent instances in which one parent of an affected child had mild features consistent with previously unsuspected AGS. Though most AGS patients have normal karyotypes, many cases of interstitial deletions have indicated that the locus for AGS lies at 20p12 (refs 6–10). A linkage analysis in a three-generation AGS family with no visible cytogenetic deletion confirmed the localization to 20p12 and positioned AGS between *D20S59* and *D20S65*[11]. Two AGS families with apparently balanced translocations in this region of chromosome 20 have been reported[12,13]. The current centromeric boundary, *D20S186*, was identified by the analysis of one of these translocation patients with t(2;20)(q21.3;p12)[12,14]. Hopes that these translocations would precisely locate the AGS gene were dimmed by the discovery that significant 20p deletions are present in both instances[14] (T.O., unpublished data). Fluorescent *in situ* hybridization (FISH) analysis of the chromosomal deletion in another AGS patient previously defined the gene *SNAP* (synaptosomal-associated protein) as the telomeric boundary for the AGS interval[15,16]. Therefore, the current critical region for the AGS gene is bounded by the markers *SNAP* and *D20S186*, representing roughly a 1.3-Mb interval within a 3.7-Mb YAC clone contig reported for this region[17].

In this report, we further narrow the AGS interval to a 250-kb region on the basis of deletions in two AGS patients. Focusing on a CpG island located in this critical region, we recently isolated a cDNA from the human *Jagged1* (*JAG1*) gene[18]. We have now determined the complete exon–intron structure of *JAG1* and used this information to identify a number of frame-shift and splice donor mutations in *JAG1* in individuals with AGS. The role played by Jagged1 as a ligand for the Notch family of proteins adds to the potential significance of this observation.

Bacterial artificial chromosome clone contig for the AGS critical region

Three overlapping YAC clones (Fig. 1*a*) spanning the 1.3 Mb AGS critical region were identified from the 3.7-Mb YAC clone contig[17]. To facilitate the process of deletion analysis and gene hunting, we generated a bacterial artificial chromosome (BAC) clone contig for the telomeric half (600 kb) of the AGS critical region. Initially, seven BAC clones (b278A8, b173K6, b255F12, b279K16, b204H22, b365D23 and b334G22) were isolated by screening with a total of six STSs. These included *D20S505* and *D20S507*, two ESTs for *SNAP* (WI-7829 and WI-6063) and two STSs generated from the 5' (J-1) and 3' (B-2) regions of the *JAG1* cDNA (Fig. 1*b*; Table 1). Eight additional STSs were generated by sequencing the ends of these BAC clones (Table 1), and these were subsequently used to screen the

[1]*Laboratory of Gene Transfer,* [2]*Laboratory of Cancer Genetics, National Human Genome Research Institute, National Institutes of Health, Bethesda, Maryland 20892-4442, USA.* [3]*Department of Pediatrics, Nagoya City University, Medical School, Nagoya 467, Japan.* [4]*Children's Hospital of Philadelphia, Philadelphia, Pennsylvania 19104-4399, USA.* [5]*Research Genetics Inc., Huntsville, Alabama 35801, USA. Correspondence should be addressed to F.S.C. e-mail: fc23a@nih.gov*

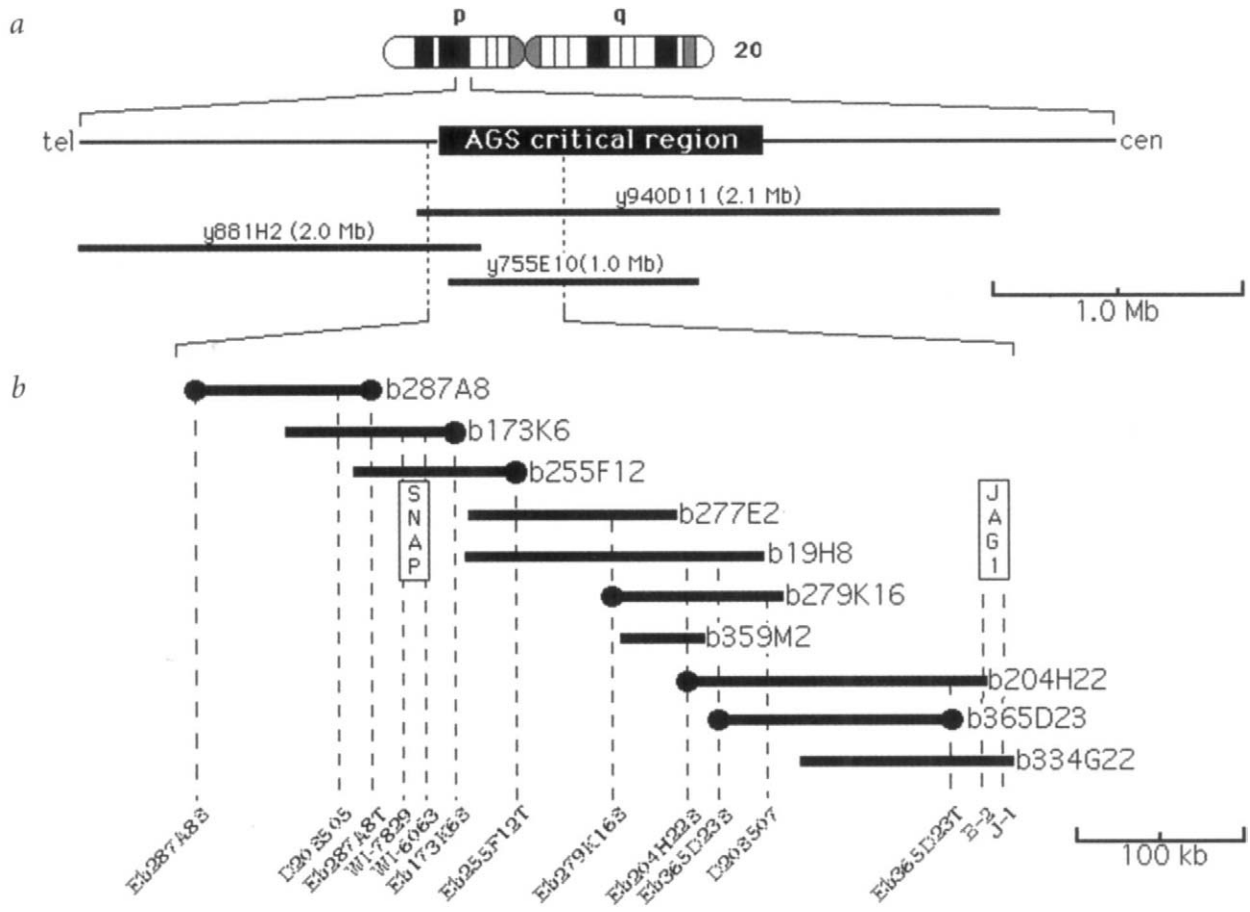

Fig. 1 Physical maps of the Alagille syndrome (AGS) critical region at 20p12. ***a***, Three overlapping YAC clones (y881H2, y755E10 and y940D11) cover a region of 3.5 Mb, and include the previously defined 1.3-Mb AGS critical region. ***b***, A contig for the telomeric half of the AGS critical region consists of 10 BAC clones (names with prefix 'b') and 14 STSs (shown at the bottom). The presence of an STS in a BAC clone is shown by the dashed line connecting the STS to the clone. The STSs derived from the end sequence of the BAC clones (filled circles at the end of the clone) begin with E, followed by the clone name and ending with a letter 'T' or 'S' to indicate whether the STS was derived from the T7 or the SP6 end of the clone. The locations of two genes, *SNAP* and *JAG1*, are indicated.

BAC library, resulting in the isolation of three additional BAC clones (b277E2, b19H8 and b359M2). The sizes of the BAC clones ranged from 50 to 225 kb, and none were found to be chimaeric.

Narrowing the AGS critical region to 250 kb

Metaphase chromosomes from five AGS probands without visible cytogenetic alterations of 20p were analyzed for submicroscopic deletions by FISH analysis using overlapping BAC clones representing the 600-kb contig as probes. In kindred A, the proband showed complete loss of one allele for BAC clones b255F12 and b204H22 and a reduced signal for b334G22 (Fig. 2*a–c*). This indicated that the centromeric breakpoint of the deletion in kindred A lies within the BAC clone b334G22 but centromeric to the clone b204H22. The location of the breakpoint in b334G22 was further supported by two observations: 1. The polymorphic marker *D20S1154* (see below), present in both b334G22 and b204H22, identified loss of an allele in this patient (data not shown). 2. Southern analysis of DNA from this patient using a probe from the 3' half of the *JAG1* cDNA (see below), shared by both b334G22 and b204H22, showed half the intensity of control DNA, indicating

Table 1 • PCR primer sequences of STSs used to construct the BAC contig

STSs	Sense primer sequence	Antisense primer sequence	Size (bp)
J-1	TCAAAGAAGCGATCAGAATAATAAAAGGAGGC	GCCGATTGGAGCATGCACGACTGGAAA	119
M-1	TGGCAAGGCCTGTACTGTGATAA	CCTGGGGAACACTCACACTCAA	979
B-2	CATAGCATTGTAAGCGTATGGC	AATCCTCAAACTGCCTCAGTC	228
Eb287A8S	ATGCAAAGGAACACCGGAGC	GCTCTGGCTCCCCGACCTT	111
Eb287A8T	CTGGGAGGAGAATAACATTTTGAGT	TGAGGATTCTGTCATTGGTGGAT	144
Eb173K6S	TTTGCCTGGTTTCCCTTATTATCA	ACTTCCCCAAATGTTACTATGAGCC	120
Eb255F12T	AGCACTTTAAACTCCTACAATAATGAATA	CCCAAGTAATGCGGCTGAT	302
Eb279K16S	GTTTTACCGGAATCCAGCCACTC	TGCCACCGCACTCCAACCT	245
Eb204H22S	GGATGGGGTAGCGATTGAGA	TGCTGTACGTTTTTGCCATTTC	94
Eb365D23S	GAAATTTGCCTAGGGTCACAGAG	ACCTCATCCCAATCTTCTCCTGC	153
Eb365D23T	AAGGAATACCTTGGGCGTTG	ATTGCCGAGGCCTCATCACTA	70
D20S1154	CTAAGACCGCTTTCCCTGTTGA	ACTTGCATTTTAAACACAATCCCTG	205

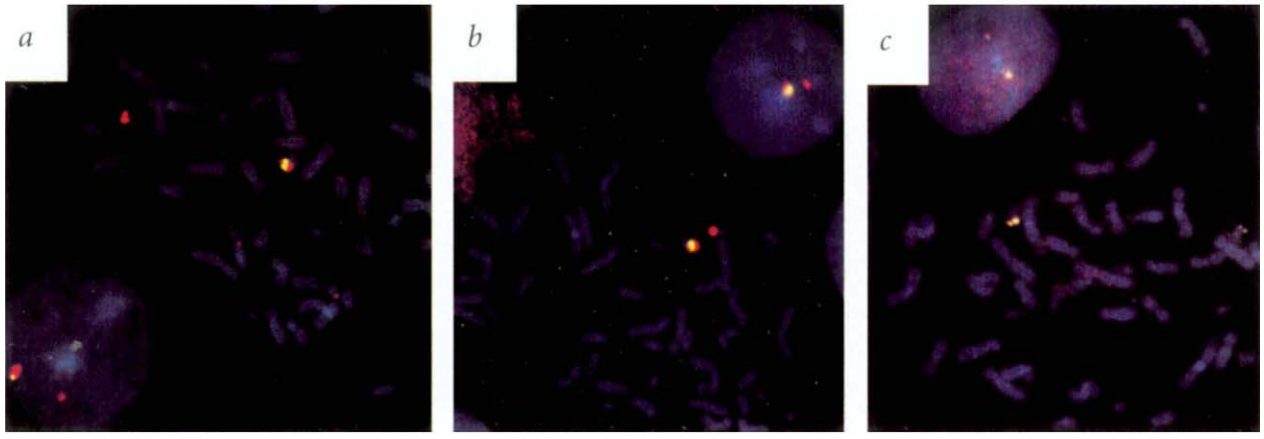

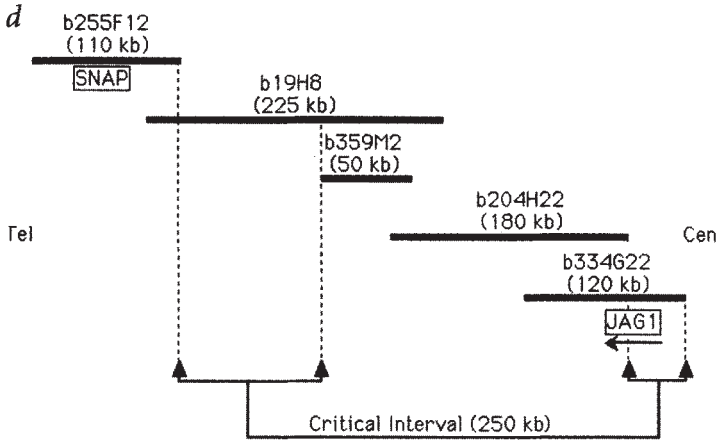

Fig. 2 Identification of a submicroscopic deletion in kindred A by fluorescent *in situ* hybridization (FISH). FISH analysis with a YAC and three BAC clone probes on interphase and metaphase chromosomes on the proband is shown here. YAC y881H2 is labelled with spectrum orange–dUTP (red signal), and BACs are labelled with biotin-dUTP (green signal). A yellow signal indicates coincident localization of both probes. The BAC probes are ***(a)*** b255F12, ***(b)*** b204H22 and ***(c)*** b334G22. It is apparent that BACs b255F12 and b204H22 are deleted in one chromosome 20, and the signal from b334G22 is reduced. The intensity of the signal from YAC y881H2 is also reproducibly decreased compared to the normal homologue. The deduced centromeric break-point of the deletion indicating the new boundary on the BAC contig is shown (*d*). A new telomeric boundary in b19H8 (between b255F12 and b359M2) was identified by FISH analysis of a second patient (see text).

deletion of this region (data not shown). The telomeric boundary of the deletion in kindred A lies within YAC y881H2 (Fig. 1*a*), as a FISH signal from y881H2 is present in the deleted chromosome—albeit with reduced intensity (Fig. 2*a–c*). The telomeric breakpoint of the deletion was further delineated to lie within a BAC clone (b356O5) that maps telomeric to b255F12 but within the YAC clone y881H2 (data not shown), defining the deletion in this proband to a size of roughly 600 kb. The deletion is inherited, since the same deletion was present in the affected mother (data not shown).

This new definition of the centromeric boundary eliminates nearly a megabase from the previous AGS critical region, reducing it to about 350 kb, flanked by *SNAP* and the centromeric end of b334G22 (Fig. 2*d*). Of course, the definition of the critical region on the basis of deletion studies should also take into account that the disease-causing gene, although most likely to lie within the deleted region, may also lie nearby but have its expression affected at a distance by the deletion.

The known telomeric boundary at *SNAP* in another AGS microdeletion patient[15,16] was further analyzed, utilizing the BAC clones as probes for FISH. It was observed that b359M2 was completely deleted and b255F12 was retained, and signal from b19H8 was partially reduced (data not shown). This demonstrated that the telomeric breakpoint of the deletion in this patient lies between b255F12 and b359M2, and within b19H8. This further reduced the AGS critical region to about 250 kb (Fig. 2*d*).

JAG1 lies within the new critical interval

We recently reported the cloning and sequencing of a full-length *JAG1* cDNA from 20p12[18]. The cDNA (GenBank accession number AF003837) is 5,942 bp long and possesses three alternative polyadenylation sites. Northern blot analysis of RNA from adult tissues indicated that *JAG1* was widely expressed in many tissues. Most abundant expression was observed in ovary, prostate, pancreas, placenta and heart. Somewhat lower levels were seen in colon, small intestine, spleen and skeletal muscle, and the lowest levels in testis, thymus, leukocyte, kidney, liver and lung[18]. As b204H22 is completely deleted in kindred A, and all of the *JAG1* gene except the first five exons (see below) is present in this BAC clone, one can conclude that most or all of the *JAG1* cDNA lies in the 250-kb AGS critical region (Fig. 2*d*). Especially in light of the proposed role of its protein product as a Notch1 ligand, *JAG1* represented an attractive candidate gene for this disorder. However, analysis of AGS proband DNA samples digested with two enzymes (*Hin*dIII and *Taq*I) did not demonstrate any variant bands on Southern blot analysis, with the entire cDNA used as a probe.

Genomic structure of *JAG1*

In order to carry out mutational analysis at a higher resolution, the genomic structure of the *JAG1* gene was determined.

A cosmid library was constructed from BAC b334G22. Ninety-six colonies were screened by PCR with three STSs from the 5' end (J-1), middle (M-1) and 3' end (B-2) of *JAG1*. Two thirds of the cosmids were positive for one or more STSs. However, no single cosmid clone was positive for both the 5' and the 3' end of the gene. Two overlapping cosmids encompassing the entire *JAG1* transcript were used to generate a phage library (in M13) and a pBluescript plasmid library (pBS II; Stratagene, La Jolla, CA). Thirty-six phage clones and nine plasmid clones were identified by hybridization screening and sequenced. Direct sequencing of the cosmid DNA with primers designed from the cDNA sequence was carried out to obtain three remaining exon–intron junction sequences.

The sequence analysis indicated that *JAG1* stretches across 36 kb and has 26 exons ranging in size from 28 bp to 2,284 bp (Fig. 3). Intron sizes vary from 89 bp to nearly 9 kb.

Table 2 • Primers for SSCP analysis of the JAG1 coding region

Exon	Position of PCR product 5' end on cDNA	Sense primer sequence	Position of PCR product 3' end on cDNA	Antisense primer sequence	Product size (bp)
1	330	TCCAATCGGCGGAGTATATTAGAGC	540+40	AGAGGACGGCTGGGAGGGA	251
2	541-31	GCGCTGACCTACCTCCTTCCCT	822	CACGATGCGGTTGCGGTC	313
	767	GGGGCAACACCTTCAACCTCA	846+52	CCAGGCGCGGGTGTGAG	132
3	847-177	AAGGAAGGGGAGTTGGTTTG	898+28	GAGAAAAGTCCACAGAAGCGATAC	257
4	899-52	GGGAAGAAGGCTGCAATGTGAATA	1067	CTGGGGCGGCAGAACTTATTG	221
	1016	CCTGTGATGACTACTACTATGGCTTTGG	1153+50	GACACTAAAAGCAACAGGCACACG	188
5	1154-36	GCAGTGTGCTGACACGCCCT	1214+84	AAGAGGCATAGTCACAATAAAGTCAGTTCC	181
6	1215-34	AAGGCTAACCTGGAGGTGTGCTG	1345+33	TCCCACCCTGGGTCTCATCC	198
7	1346-53	TGGGTTCGCCATCTTCACAGG	1465+185	TCAGCATCACCCAAAAAACTTTAGAGA	358
8	1466-34	CATCCCTCTCTGACTGCCATCC	1579+69	ACCTCTCCCCAACGTGGTATCTT	217
9	1580-40	TGAATTAAATTGTCAACCCCCTCCTT	1693+36	TTGGTATAAAAATTACAGTCACAGGGATG	190
10	1694-27	CTCATGCTCATCCCCATCTCCTT	1807+56	CAGCAAGTCGGCTACCCAAGTTT	197
11	1808-45	CACTGTAAATTACCTCTTTAAAATGATGAC	1854+78	GAGCTCTCCTAGTGTCGCACAAATCT	170
12	1855-69	TGAAGCCCTGTGTTTGTGGAATAC	2028+75	GAAAAGTAAAGGGAAGCGGAGGAG	318
13	2029-34	CCCTCCCCCTTTTCGCTGTT	2179+58	AAGTGGGGACAAAAGGAGCAAGT	243
14	2180-55	GAATGCCGCATCTGTGGGTG	2344+43	AGGCTGGGGAGCACTGGTC	263
15	2345-89	AGGAGGGAGCCATGAAAACTGC	2458+48	CAACATGACCCATACATCCCAGAG	251
16	2459-52	GTGAATGGTCCTGGATCTCGTCTT	2572+66	GCCCCCTCCCACAGAAGACAG	232
17	2573-38	GGGGCCACTGGGACTCACAC	2686+71	CCAGGGGCCAACCAGCAGA	223
18	2687-85	GATATTTCTCTGGGCCTGGTTCTTG	2803+36	CCGACAGCCCTGGGAGAGTT	238
19	2804-55	GGCTAAGACCGCTTTCCCTGTT	2831+43	ACGATAGTGGATGAGTGCTGGCTT	126
20	2832-50	AGAGTAATGGACTGGGAGGTTGGTAA	2917+56	AGGCATGGAATGAAGCGGTAAAG	192
21	2918-35	CATCAGTCCCTAAACTTGAACTCCATT	3031+47	CGCTCACCCCAGAAGACCCAT	196
22	3032-95	GGCACAGGCATAACCATTTCATAA	3141+26	GAACTGCGGCAGCCATCAT	231
23	3142-78	TGGCTGCCGCAGTTCACCT	3364	TCTCCTTGTTAAAGGTAAATGTGATGTTC	301
	3263	AGTGTCGGTCTTCCAGTCTCCAG	3375+46	CAAGCAGACATCCACCATTCAAAA	159
24	3376-42	TCTCAATCTTACACGTGTGTGGGTTT	3507+36	ATCGAATAATGAGGTGTGAATGGGTC	210
25	3508-65	AATTTTGAAGAAAGGCTGCTTTGAGTAT	3658+80	CCTCGACCTGATGGCTTTATTGAA	296
26	3658-37	TCTTGGAGAGTTAATTGGTTTTGTGC	3871	CCTTGATGGGGACCGTGTTG	250
	3813	GCTGAACCAGATCAAAAACCCCA	4051	TTGTCCAGTTTGGGTGTTTTGTCG	239
	3982	GCGTATACGCTGGTAGACAGAGAAGA	4177	GACAGTTTAAAGAACTACAAGCCCTCAGA	196

Sequence from intron 19 revealed the presence of a CA dinucleotide repeat (Fig. 3*b*). Analysis of 60 chromosomes with primers designed to amplify the repeat region identified 12 alleles with heterozygosity of 85.8% and PIC of 0.844. This highly polymorphic marker, *D20S1154*, should thus be quite useful for the detection of submicroscopic deletions. In kindred A, the affected mother and offspring were found to be hemizygous for different alleles at *D20S1154*, demonstrating that the deletion identified by FISH analysis includes at least the 3' portion of *JAG1* (data not shown).

Mutation analysis of AGS probands by SSCP

A total of 31 PCR reactions were utilized to amplify the complete coding region of *JAG1* (3,657 bp). Each exon was amplified individually, and exons larger than 200 bp were amplified as multiple, overlapping products. DNA samples from seven non-deletion AGS kindreds were analysed by SSCP for the coding region of *JAG1*. Table 2 lists the primers employed for amplifying exonic regions from genomic DNA.

Fig. 4 displays three SSCP variant patterns and the accompanying sequence results, identifying a deletion, an insertion and a splice donor mutation in three unrelated AGS patients. In kindred C, a frame-shift due to a 2-bp (GT) deletion in exon 22 (3098delGT) was identified in the proband, her mother and her sister. In kindred D, both the proband (D-1) and the reportedly clinically unaffected father (D-2) showed an extremely subtle variation in the SSCP band pattern and were found to have a single nucleotide insertion (3060insG) in exon 22. In kindred E, an SSCP variant band unique to the affected offspring (Fig. 4*c*) was found to be due to a mutation changing the normal splice donor signal GT to CT (3375+1G→C) at the junction of exon 23 and intron 23.

Table 3 • Summary of JAG1 mutations identified in Alagille syndrome patients

Proband	Affected organ systems					Mutation*
	Liver	Heart	Vertebra	Face	Eye	
A[1]	+	+	+	+	+	del600kb
B	+	+	+	+	+	1950del4
C[2]	+	+	nd	+	nd	3098delGT
D[3]	+	+	–	+	–	3060insG
E	+	+	–	+	+	3375+1G→C
F[4]	+	+	nd	+	+	1345+2T→G
G	+	+	nd	+	nd	1854G→T[5]

*Mutations were designated on the basis of Beaudet and Tsui[37]. +Characteristic abnormalities present in this organ system. – No abnormality noted in this organ system. nd = not described. [1]No additional clinical features are observed in this proband with 600-kb deletion, although the affected mother may have had mild learning disability. [2]Mother and sister carry same mutation as proband but were not previously diagnosed as affected; mother is said to have suggestive facial features of AGS. [3]Father of proband carries same mutation but is reportedly clinically unaffected. [4]Mutation is found in both of male affected identical twins, but not in either of the clinically unaffected parents. [5]Possible splice alteration leading to loss of this allele at the RNA level. See text.

Table 3 summarizes the results of mutation analysis and the characteristic clinical features of seven kindreds in which *JAG1* mutations were found. The locations of mutations with respect to the structural domains of the *JAG1* encoded protein are shown in Fig. 5. Kindred A contains a 600-kb deletion, as described in Fig. 2. In kindreds B–G, three frame-shift and three splice donor mutations were identified. In addition to the mutations shown in Fig. 4, a 4-bp deletion (1950del4) in exon 12 was identified in the proband of kindred B, and a splice donor change from GT to GG (1345+2T→G) in intron 6 was found in affected identical twins in kindred F; neither parent carried this mutation.

The mutations seen in kindreds B–G were not observed in nearly 30 normal chromosomes analysed. In kindred G, a G→T change

a

Exon/ Intron	Exon length (bp)	Starting position in cDNA	Acceptor splice site*	Donor splice site*	Intron# length (bp)
1	540	1		...AGCCAAG/gtaggag	~500
2	306	541	ttccctcgccggcag/GTGTGTG...	...CTGGCCG/gtgagtg	~9000
3	52	847	ttgtttgtcttgcag/AGGTCCT...	...ACCGTTC/gtaagta	~6000
4	255	899	ccactttgtctctag/AACCTGA...	...AACAGAG/gtatgtg	~2000
5	61	1154	ctctgtttttttacag/CTATTTG...	...ACTGCAG/gtaaatc	~4000
6	131	1215	gctgtgtgtctccag/GTGCCAG...	...GACAAAG/gtatggc	217
7	120	1346	ggatctttttggcag/ATCTCAA...	...GAAATTG/gtaagtg	436
8	114	1466	tcctggtttttgcag/CTGAGCA...	...TCTACAA/gtaagtc	~1200
9	114	1580	tttcttgttgaccag/ACATTGA...	...CAGTTAG/gtaagaa	~650
10	114	1694	cccatctcctttcag/ATGCAAA...	...GACATAA/gtgagtg	413
11	47	1808	ttatttatttttag/ATATTAA...	...CTGTCGG/gtatgta	~400
12	174	1855	cttctcctcttctag/GATTTGG...	...CTGTCAG/gtgagtg	~500
13	151	2029	tcatgatatttgcag/CTGGACA...	...TGTGAAG/gtacctc	~900
14	165	2180	aagcctatcttctag/TGATTGA...	...CATGAAA/gtaagac	~1000
15	114	2345	tactttgtttcatag/ATATTAA...	...GAAACCA/gtgagtc	~550
16	114	2459	ccccttttgattctag/ATATTAA...	...CACTCAC/gtaagtg	99
17	114	2573	aatattttcctccag/GTGACAG...	...AACATAG/gtaactt	163
18	117	2687	gctcttcttttatag/CCCGAAA...	...GCTCAGA/gtgtcct	~500
19	28	2804	gtcttttctttgcag/ATACCAA...	...ATCCCTG/gtaagtg	~600
20	86	2832	tctttgctttcttag/TTACAAC...	...AGAATAA/gtaagga	~1200
21	114	2918	ctccatttctcctag/ACATCAA...	...CAGGAAG/gtatgtg	~650
22	110	3032	gtctccacctgtcag/TTTCAGG...	...CTCAAAG/gtaggac	89
23	234	3142	tctgtttttctccag/GTCTGGT...	...GTCACCA/gtatgta	209
24	132	3376	taaaaatcgttttag/GGTCTTA...	...GGCCATT/gtaagta	180
25	151	3508	caattgtttttccag/TCTGCTG...	...AGAACAG/gtaggtg	~900
26	2284	3659	gtgcctgccttacag/ATTTCCT...		

* The exonic and intronic sequences are in upper-case and lower-case letters, respectively. #The size of introns marked '~' indicates the size deduced from products obtained from primers in adjacent exons.

b

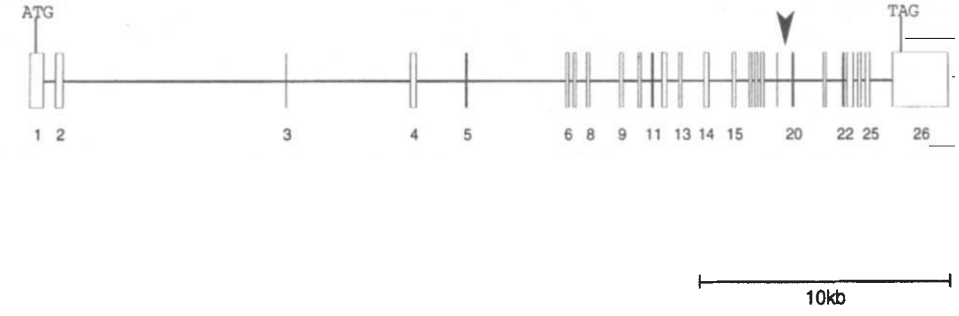

Fig. 3 Exon–intron organization of *JAG1*. ***a***, Sizes and location of the exons and introns, and nucleotide sequences of splice acceptor and donor sites are shown. ***b***, Diagrammatic representation of the exon–intron organization of the *JAG1* gene. Exons are indicated by open rectangles and are numbered. The location of the start codon ATG (exon 1) and the termination codon TAG (exon 26) are indicated. The arrowhead points to the location of the polymorphic microsatellite marker (*D20S1154*) in intron 19.

in the last nucleotide of exon 11 (1845G→T) initially appeared to be a silent mutation, since this substitution changes the codon from CGG to CGT, both of which code for arginine. However, this sequence alteration occurs immediately upstream of the junction of exon 11 and intron 11, changing this from GTCGG/gtatgt to GTCGT/gtatgt. None of the 100 chromosomes from normal subjects showed this sequence variation. We hypothesized that this sequence change might either interfere with utilization of the normal splice donor (G is the preferred final nucleotide before the gt splice donor) or even create a new splice donor (GTgtat is almost as good a match to the consensus donor sequence of GTRAGT as the normal splice donor gtatgt).

To test this hypothesis, we analysed RT-PCR products from a fibroblast cell line from this proband, using primers in exons 10 and 12 to amplify *JAG1* cDNA. In contrast to the genomic DNA, the cDNA contained only the wild-type nucleotide (G) at the last position of exon 11 (data not shown). No evidence was found in the cDNA for the variant (T) nucleotide, a product skipping exon 11, or a product corresponding to utilization of the proposed new splice donor. Thus, the allele containing the 1845G→T mutation is apparently not stably expressed in this patient. We cannot currently distinguish whether this is due to (1) interference with utilization of the normal splice donor, resulting in aberrantly spliced and unstable RNA that is rapidly degraded; (2) creation of a new splice donor, resulting in an RNA containing a 2-bp deletion that is unstable; or (3) an undetected independent mutation in *cis* to the G→T substitution that abolishes RNA expression from this allele.

Discussion

Given the occasional observation of patients with visible cytogenetic deletions of 20p, Alagille syndrome has been proposed as a possible contiguous gene deletion syndrome[10,19–21]. But a recent study employing a panel of six microsatellite markers within the 1.9-Mb minimal AGS region identified only a single case of a submicroscopic deletion out of 24 patients[22]. This suggested the more likely possibility that AGS is due to loss-of-function mutations in a single gene. The data reported here and in the accompanying study[23] now leave little doubt that this interpretation is correct, and that mutations in *JAG1* alone are sufficient to produce all the characteristic features of AGS.

Centromeric and telomeric boundaries of AGS deletions have previously defined a 1.3-Mb minimal interval between *SNAP* and *D20S186*[14–16]. In this work, we were able to narrow this interval substantially by constructing a physical contig and determining narrower boundaries for two deletion patients by using FISH. On the telomeric side, it was possible to reduce the candidate interval by about 100 kb by re-analysis of a previously described patient[15,16], and on the centromeric side a newly described 600-kb deletion in kindred A allowed nearly a megabase of the previous candidate interval to be excluded. A complete BAC contig of this 250-kb minimal interval was generated.

Within this interval we identified a gene that showed high homology with the rat gene *Jagged1*, which encodes a ligand for the Notch family of receptors[18]. Determination of the complete exon–intron structure allowed screening all 26 exons and the exon–intron boundaries for the presence of mutations in AGS patients.

The results (Table 3) leave little doubt that heterozygous mutations that abolish function of one allele of *JAG1* lead to AGS. Of the AGS patients in whom the gene sequence was thoroughly investigated, only one failed to reveal a mutation. Particular confidence in the identification of *JAG1* as the AGS gene is provided by kindreds E and F, in which new mutations in invariant splice donor sequences coincide with the appearance of the disorder in the family.

Given that the phenotype of patients with submicroscopic dele-

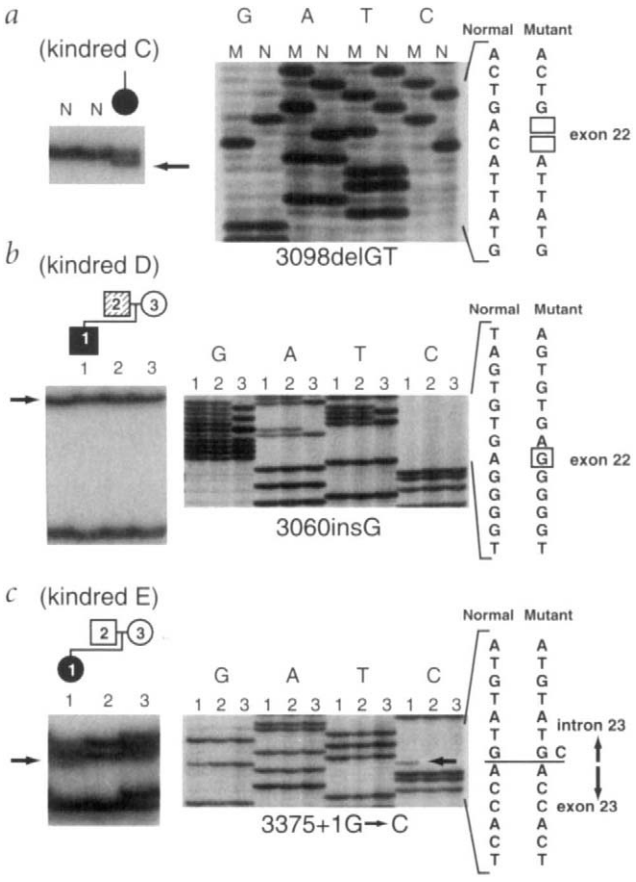

Fig. 4 Mutation detection in three AGS kindreds by SSCP and sequence analysis. ***a,*** Kindred C. An SSCP variant band from exon 22 was excised, re-amplified and directly sequenced. The antisense strand sequence of the mutant and a normal allele are shown, demonstrating the 3098delGT mutation. ***b,*** Kindred D. Here the SSCP changes in individuals D-1 and D-2 were extremely subtle, and it was not possible to excise the variant band clearly from the normal allele. Sequencing revealed only wild-type sequence in lane 3 (the mother), whereas lanes 1 and 2 (proband and father) demonstrate a mutation with an insertion of G (3060insG) along with the wild-type sequence. ***c,*** Kindred E. A common polymorphism is present in intron 23 (9 Ts vs 10 Ts, beginning 18 nt into the intron, with allele frequencies based on the analysis of 64 chromosomes being 28% and 72%, respectively) and accounts for the SSCP difference between E-2 and E-3. But the appearance of a new SSCP band (arrow) in the proband (E-1) suggested a new mutation. Sense strand sequence of the PCR product amplified from genomic DNA confirms this, demonstrating the presence of both G and C nucleotides in the proband, whereas the unaffected parents show only the expected G at the first nucleotide position of intron 23.

tions (as in kindred A) or loss of expression of the mutant allele (as in kindred G) does not seem reproducibly different from that with frame-shift and splice alterations of *JAG1* (Table 3), the most conservative interpretation of these observations is that AGS is caused by haploinsufficiency of the protein product of this gene. While a dominant negative role for a truncated protein cannot be ruled out, it does not seem necessary to invoke this. Patients with larger, cytogenetically visible deletions can have an expanded phenotype, including developmental delay and hearing loss[24], but the cardinal features of AGS (including liver, heart, eye, vertebral and facial findings) can apparently be attributed to mutations in *JAG1* alone. It is probably premature to draw other conclusions about genotype–phenotype correlations in AGS, although analysis of larger numbers of patients will be of great interest. Such correlations will be confounded, however, by profound differences in phenotype within a given family (as exemplified by kindreds C and D), indicating that factors not attributable to the specific *JAG1* mutation must play a major role in determination of the phenotype.

The Notch family of receptors has been identified to play a critical role in development in organisms from *C. elegans* to mammals. In a process known as lateral specification, identical precursor cells during early development must choose between alternative cell fates, mediated by direct cell–cell contact. A well-studied example is the formation of the *Drosophila* peripheral nervous system[25,26]. In this case, Notch and its membrane-bound ligand, Delta, are simultaneously expressed on precursor cells that must choose between epidermal and neural fates. Loss-of-function mutations of either *Notch* or *Delta* result in extra primary fate cells (neurons) and fewer epidermal cells, leading to the conclusion that Notch signalling inhibits neural pathway differentiation.

In the mouse, four *Notch* genes have been found; for three of these, the human homologues have been cloned[26–28]. All these proteins share a basic structure of 34 to 36 extracellular EGF-like repeats, three extracellular cysteine-rich Notch/Lin-12 repeats, a transmembrane anchor and an intracellular domain containing ankyrin repeats and a PEST sequence.

Two of the human *NOTCH* genes have been implicated in disease pathogenesis. A somatic activating mutation of *NOTCH1* (denoted *TAN1*) truncating the extracellular domain was initially described as the product of a t(7;9) translocation in a T-cell leukaemia[29]; presumably, the constitutive activation of Notch1 activity resulting from this truncation promotes oncogenesis by blocking cellular differentiation and allowing continuing proliferation. Similar oncogenic effects have been observed for truncating mutations of *Notch2*, *Notch3* and *Notch4* (*Int3*) in mice.

Recently, a series of human pedigrees with cerebral autosomal dominant arteriopathy with subcortical infarcts and leukoen-

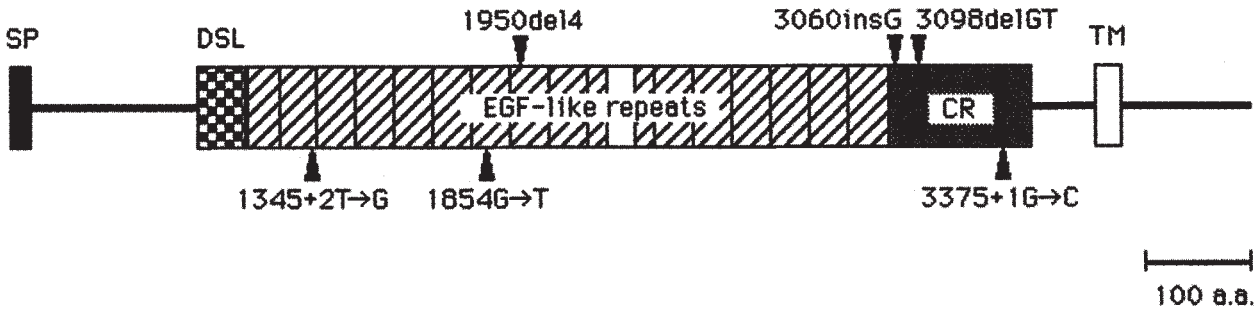

Fig. 5 Schematic representation of structural motifs in the human Jagged1 protein and locations of mutations identified in AGS patients. The signal peptide (SP), the Delta/Serrate/Lag-2 domain (DSL), the EGF-like repeats, the cysteine-rich region (CR) and the transmembrane domain (TM) are shown. The locations of three frame-shift mutations observed in kindred B (1950del4), C (3098delGT) and D (3060insG) are indicated above the diagram, and the splice donor mutations in kindred E (3375+1G→C), F (1345+2T→G) and G (1854G→T) are indicated below. Among the frame-shift mutations, 3098delGT results in a termination codon at the site of deletion (codon 880), whereas 1950del4 and 3060insG result in stop codons at 562 and 878, respectively.

cephalopathy (CADASIL), a rare cause of stroke and dementia, were discovered to harbor germline missense alterations in *NOTCH3*[30]. The severe vascular smooth-muscle cell alterations in affected members of these families were proposed to be a consequence of deranged Notch3 signalling.

In *Drosophila*, the known Notch ligands are Delta and Serrate; in *C. elegans*, they are Lag-2 and Apx-1. The complete catalogue of vertebrate ligands is still under construction[27], but it includes Jagged1, Jagged2 and Delta1 (also called Dll1, for Delta-like). All the known ligands have a common structure (Fig. 5): an amino-terminal extracellular conserved DSL (Delta-Serrate-Lag-2) domain, a variable number of EGF-like repeats, a single transmembrane domain and a cytoplasmic domain that displays no sequence similarity between different ligands. Rat Jagged1 was shown in a functional cell–cell interaction assay to activate Notch1 and inhibit muscle cell differentiation in cell culture[31]. Rat *Jagged2* has been identified by probing of a cDNA library with *Jagged1* at low stringency[32].

The expression patterns of rat *Jagged1*, *Jagged2*, *Delta1*, *Notch1*, *Notch2* and *Notch3* have been studied by *in situ* hybridization[32,33]. *Jagged1* expression was detected in E10.5 and E12.5 embryos in the first and second branchial clefts, otic vesicle, eye, midbrain, hindbrain, neural crest, spinal cord, heart and the area dorsal to the heart, forelimb bud and tail bud. No obvious correlation existed between the pattern of ligand and receptor expression, leaving open the question of whether each ligand is able to interact with each receptor.

How does this information about the Notch pathway in model organisms assist in our understanding of the AGS phenotype? First of all, one can appreciate that dosage of the various Notch ligands might well be critical for normal embryonic development; the delicate balance that must exist between ligand and receptor during cell–cell interactions that determine cell fates could understandably be upset by the presence of only 50% of the normal amount of Jagged1 protein, which is predicted to be the case in AGS. Second, the pattern of *Jagged1* expression as determined in the rat embryo bears some interesting similarities to the organ system involvement in AGS—specifically, the heart and eye are both sites of expression, and the area of maximal expression in the eye (ciliary margins of the retina)[34] roughly correlates with the observed pathology of posterior embryotoxon seen in AGS. The correlation is not precise, however; no explanation is provided by these expression studies for the prominent liver and bile duct abnormalities in AGS, although detailed analysis of *Jagged1* expression in the developing liver has not been carried out. Given the prominent role played by Notch and its ligands in nervous system development, it is perhaps surprising that the phenotype of AGS does not include more profound central and peripheral nervous system defects. This may reflect the redundancy of multiple ligands and receptors; if those redundant elements also display genetic variability in humans, one could imagine that this might account in part for the marked variable expressivity of the phenotype of AGS.

In the context of these observations, it would not be surprising if other disorders of human development turn out to be caused by dosage abnormalities of other members of the family of Notch proteins and Notch ligands. As with AGS, one might expect such phenotypes to be highly pleiotropic.

Writing more than 300 years ago, William Harvey presciently observed: "Nature is nowhere more accustomed more openly to display her secret mysteries than in cases where she shows traces of her workings apart from the beaten path; nor is there any better way to advance the proper practice of medicine than to give our minds to the discovery of the usual law of Nature by careful investigation of cases of rare forms of diseases. For it has been found in almost all things, that what they contain of useful or applicable nature is hardly perceived unless we are deprived of them, or they become deranged in some way" (quoted by A. Garrod in 'The lessons of rare maladies'[35]). Harvey could hardly have imagined the remarkable aptness of his comment for modern molecular analyses of uncommon human developmental disorders, which promise to yield a continuing harvest of interesting revelations about genes, pathways and phenotypes.

Methods

BAC contig. A human BAC library (Research Genetics, Huntsville, AL; approx. 146,000 clones, 4× coverage, average insert size 130 kb) was screened by PCR. The contig was assembled by the analysis of 12 BAC clones with 14 STSs. Sizes of BAC clones were determined by PFGE of *Not*I digested BAC DNA (1 µg), which separates the 7.3-kb vector from the insert fragment(s). All the new STSs are listed in Table 1. J-1, M-1 and B-2 were designed from the 5' end, middle and 3' end of the *JAG1* cDNA sequence. The STSs starting with E were developed from the end sequence of the corresponding BAC clones (see below).

Direct sequencing of BAC clone ends. BAC DNAs were isolated with the AutoGen 740 (Integrated Separation Systems, Natick, MA). After RNase treatment, 1 µg BAC DNA template was used in each dideoxy sequencing reaction by means of CATALYST (Taq DyePrimer reaction; PE Applied Biosystems, Foster City, CA) with primers M13F (for the T7 end) and M13R (for the SP6 end).

Exon–intron structure of *JAG1*. A cosmid library was generated from b334G22 DNA. Briefly, BAC DNA was isolated with a standard alkaline-SDS method and then twice subjected to CsCl gradient centrifugation. After partial digestion with *Sau3A*I, DNA fragments were electrophoresed on a preparative 0.8% LMP agarose gel (SeaPlaque GTG; FMC BioProducts, Rockland, ME). Fragments >23 kb were cut out from the gel, then ligated into *Bam* HI digested pWE15 vector (Stratagene, La Jolla, CA). After packaging with GigapackIII (Stratagene), XL1-Blue cells were used for plating. Resulting cosmid colonies were arrayed on a 96-well plate and screened by PCR. Two overlapping cosmid clones encompassing the entire *JAG1* gene were used to generate a M13 phage library (carried out by SEQwright, Houston, TX) and a plasmid library (using vector pBluescript II, Stratagene). Positive M13 clones detected by hybridization with a full-length *JAG1* cDNA probe, and plasmid clones identified by hybridization to end-labelled oligonucleotide probes, were sequenced. In addition, direct sequencing of the same cosmid DNAs with primers designed from the cDNA sequence was carried out to obtain three remaining exon–intron sequences (exons 4, 12 and 20). The size of introns 6, 7, 10, 16, 17, 22, 23 and 24 was determined by direct sequencing. We estimated other intron sizes from the size of the genomic DNA PCR products using primers generated specifically to amplify individual introns. PCR products >2 kb were obtained with a long-range PCR method (XL PCR kit; Perkin Elmer, Foster City, CA).

FISH analysis. Metaphase spreads were prepared from EBV-transformed lymphoblastoid cells. Total yeast DNA from the YAC clone, y881H2, was labelled with d-UTP Spectrum Orange by nick translation according to the manufacturer's directions (Life Technologies, Inc., Gaithersburg, MD). In the same way, BAC DNAs (b255F12, b204H22 and b334G22) were labelled with biotin-16-dUTP. Hybridization, washes and detection were performed by means of a standard protocol as previously described[36].

Patient DNA samples for SSCP. Mutations in seven AGS kindreds are reported in this study. Kindreds A and B, and kindreds C and F, were enrolled under the IRB approved protocols of the Nagoya City University and Children's Hospital of Philadelphia, respectively. Cell lines (fibroblast and EBV-transformed lymphoblastoid) from kindreds D, E and G were obtained from the Coriell Institute for Medical Research (Camden, NJ) (individuals D-1 to D-3, GM12079A, GM12228 and GM12227A; E-1 to E-3, GM12016, GM12018A and GM12017; G-1, GM05759). The Puregene DNA isolation kit (Gentra Systems, Inc., Minneapolis, MN) was used for DNA extraction from these cell lines.

SSCP analysis. Thirty-one PCR primer pairs were generated for the amplification of all *JAG1* exons from genomic DNA (Table 2). PCR was carried out under standard conditions containing 1 µl (20 ng) of genomic DNA template, 2 µl of 10× PCR buffer (Perkin Elmer, Foster City, CA), 2 µl of dNTP mix (2 mM dATP, 2 mM dGTP, 2 mM dTTP, 0.2 mM dCTP), 1 µl of 10-µM forward primer, 1 µl of 10-µM reverse primer, 0.1 µl of AmpliTaq DNA

polymerase (5 U/μl), 0.05 μl α^{32}P dCTP (NEN Life Science, Wilmington, DE) and 11.85 μl of ddH_2O. All amplifications were performed with a GeneAmp PCR System 9600 (Perkin Elmer). After 3 min of initial denaturing at 94 °C, the reaction cycle was performed as follows: primer annealing at 60 °C for 20 s, extension at 72 °C for 20 s and denaturing at 94 °C for 20 s. The final extension was for 3 min. One microliter of PCR product was added to 10 μl of denaturing stop solution (95% formamide, 10 mM NaOH, 0.25% bromophenol blue, 0.25% xylene cyanol), denatured 4 min at 94 °C and rapidly cooled on ice water. SSCP gels were prepared with 15 ml of MDE gel solution (FMC BioProducts), 14.4 ml of ddH_2O, 3.6 ml of 10× TBE buffer (0.89 M Tris, 0.89 M boric acid, 0.02 M EDTA), 240 μl of 10% ammonium persulfate and 24 μl of TEMED. Three and a half microliters of each reaction was loaded, and gels were run in 0.6× TBE buffer at 6 W for 9 h at room temperature. Gels were then dried under vacuum at 80 °C and exposed to autoradiography at room temperature for 6–12 h.

Direct DNA sequencing. If possible, variant SSCP bands were cut from the gels after alignment with the autoradiograph and placed directly in the PCR reactions. The reaction contained 37.5 μl ddH_2O, 5 μl of 10× PCR buffer (Perkin Elmer), 1 μl 10 mM forward primer, 1 μl of 10 mM reverse primer, 5 μl of dNTP (2 mM each) mix and 0.5 μl of AmpliTaq DNA polymerase. For the re-amplification, the bands were denatured for 1 min at 95 °C and subjected to a 30-cycle amplification. Each cycle was 20 s denaturing at 94 °C, 20 sec annealing at 60 °C and 20 s extension at 72 °C. A final extension step for 3 min at 72 °C was added. One tenth of the reaction was run in a 1.5% agarose gel to visualize yield. The amplified DNAs were then column purified with PCR-SELECT II columns (5Prime→3Prime, Inc., Boulder, CO), precipitated, and re-suspended in 10 μl of ddH_2O. The sequencing reaction was carried out with AmpliCycle Sequencing Kit (Perkin Elmer) after kinasing of the sequence primer, which is the same as the PCR primer, with γ-^{33}P using polynucleotide kinase (Boehringer Mannheim Co., Indianapolis, IN). Reaction products were denatured for 3 min at 94 °C with stop solution, placed on ice for 2 min, then electrophoresed on a 6% sequencing gel (GEL-MIX 6; Life Technologies) for 1.5–2.0 h in 1.0× TBE buffer. Gels were dried under vacuum at 80 °C after fixing with 10% methanol and 10% acetic acid solution, and then exposed to autoradiography film at room temperature for 12 h.

RNA isolation and RT-PCR. RNA was isolated from cell lines with TRISOL Reagent (Life Technologies) according to the manufacturer's instructions. Total RNA (1 μg) isolated from patient's cell lines was used for synthesizing single-strand cDNA with *JAG1* gene-specific antisense oligonucleotide from exon 26 (5507th to 5534th nt on *JAG1* cDNA (5'–CATTGAGACCGTGAAGATACTTTGTATT–3') using reagents from the 5' RACE System (Life Technologies). For kindred G, the amplification of exon 11 from RT-cDNA was carried out with one primer generated from the 3' end region of exon 10 (5'–GCTACTACTGCGACTGTCTTCCCG–3') and the other from the 5' end region of exon 12 (5'–CCAGGTGGACAGATACAGCGATAA–3') in PCR. Reaction was carried out in 40 cycles to amplify enough product for analysis. The PCR products were sequenced as described above.

Acknowledgements

We deeply appreciate the participation of AGS patients and families in this study. We thank K. Nishio and K. Sugiyama for clinical care of the patients. Assistance from Y. Miyake in establishing cell lines, R. Walker and N. Dietrich for DNA sequencing, and D. Leja for preparing illustrations is gratefully acknowledged.

Received 29 April; accepted 6 June 1997.

1. Alagille, D., Odievre, M., Gautier, M. & Dommergues, J.P. Hepatic ductular hypoplasia associated with characteristic facies, vertebral malformations, retarded physical, mental and sexual development, and cardiac murmur. *J. Pediatr.* **86**, 63–71 (1975).
2. Alagille, D. *et al.* Syndromic paucity of interlobular bile ducts (Alagille syndrome or arteriohepatic dysplasia): review of 80 cases. *J. Pediatr.* **110**, 195–200 (1987).
3. Danks, D.M., Campbell, P.E., Jack, I., Rogers, J. & Smith, A.L. Studies of the aetiology of neonatal hepatitis and biliary atresia. *Arch. Dis. Child* **52**, 360–367 (1977).
4. Dhorne-Pollet, S., Deleuze, J.F., Hadchouel, M. & Bonaiti-Pellie, C. Segregation analysis of Alagille syndrome. *J. Med. Genet.* **31**, 453–457 (1994).
5. Elmslie, F.V. *et al.* Alagille syndrome: family studies. *J. Med. Genet.* **32**, 264–268 (1995).
6. Byrne, J.L., Harrod, M.J., Friedman, J.M. & Howard-Peebles, P.N. Del(20p) with manifestations of arteriohepatic dysplasia. *Am. J. Med. Genet.* **24**, 673–678 (1986).
7. Anad, F. *et al.* Alagille syndrome and deletion of 20p. *J. Med. Genet.* **27**, 729–737 (1990).
8. Legius, E. *et al.* Alagille syndrome (arteriohepatic dysplasia) and del(20)(p11.2). *Am. J. Med. Genet.* **35**, 532–535 (1990).
9. Teebi, A.S., Murthy, D.S., Ismail, E.A. & Redha, A.A. Alagille syndrome with de novo del(20)(p11.2). *Am. J. Med. Genet.* **42**, 35–38 (1992).
10. Deleuze, J.F., Hazan, J., Dhorne, S., Weissenbach, J. & Hadchouel, M. Mapping of microsatellite markers in the Alagille region and screening of microdeletions by genotyping 23 patients. *Eur. J. Hum. Genet.* **2**, 185–190 (1994).
11. Hol, F.A. *et al.* Localization of Alagille syndrome to 20p11.2-p12 by linkage analysis of a three-generation family. *Hum. Genet.* **95**, 687–690 (1995).
12. Spinner, N.B. *et al.* Cytologically balanced t(2;20) in a two-generation family with Alagille syndrome: cytogenetic and molecular studies. *Am. J. Hum. Genet.* **55**, 238–243 (1994).
13. Hattori, M. *et al.* Alagille syndrome with t(3;20)(q13.3;p12.2). *Nippon Shonika Gakkai Zasshi* **99**, 1984–1986 (1995).
14. Spinner, N.B. *et al.* Defining the Alagille syndrome critical region on 20p using a translocation breakpoint and overlapping deletions. *Am. J. Hum. Genet.* **57**, A35 (1995).
15. Krantz, I.D. *et al.* Investigation of SNAP-25 and PLCB4 as candidate genes for Alagille syndrome. *Cytogenet. Cell. Genet.* **74**, 304–304 (1996).
16. Krantz, I.D. *et al.* Narrowing of the Alagille syndrome critical region and analysis of SNAP as a candidate gene. *Am. J. Hum. Genet.* **59**, A224 (1996).
17. Pollet, N. *et al.* Construction of a 3.7-Mb physical map within human chromosome 20p12 ordering 18 markers in the Alagille syndrome locus. *Genomics* **27**, 467–474 (1995).
18. Oda, T., Elkahloun, A.G., Meltzer, P.S. & Chandrasekharappa, S.C. Identification and cloning of the human homolog (*JAG1*) of the rat *Jagged* gene from the Alagille syndrome critical region at 20p12. *Genomics* (in the press).
19. Schnittger, S., Hofers, C., Heidemann, P., Beermann, F. & Hansmann, I. Molecular and cytogenetic analysis of an interstitial 20p deletion associated with syndromic intrahepatic ductular hypoplasia (Alagille syndrome). *Hum. Genet.* **83**, 239–244 (1989).
20. Desmaze, C. *et al.* Screening of microdeletions of chromosome 20 in patients with Alagille syndrome. *J. Med. Genet.* **29**, 233–235 (1992).
21. Deleuze, J.F. *et al.* Deleted chromosome 20 from a patient with Alagille syndrome isolated in a cell hybrid through leucine transport selection: study of three candidate genes. *Mamm. Genome.* **5**, 663–669 (1994).
22. Rand, E.B., Spinner, N.B., Piccoli, D.A., Whitington, P.F. & Taub, R. Molecular analysis of 24 Alagille syndrome families identifies a single submicroscopic deletion and further localizes the Alagille region within 20p12. *Am. J. Hum. Genet.* **57**, 1068–1073 (1995).
23. Li, L. *et al.* Alagille syndrome is caused by mutations in *Jag1*, a ligand for Notch1. *Nat. Genet.* **16**, 243–251 (1997).
24. Spinner, N.B. *et al.* Mapping the Alagille syndrome critical region within 20p12. Proc. Single Chromosome 20 Workshop, February 1997, Hinxton, Cambridgeshire, UK *Cytogenet. Cell. Genet.* (in the press).
25. Heitzler, P. & Simpson, P. The choice of cell fate in the epidermis of Drosophila. *Cell* **64**, 1083–1092 (1991).
26. Artavanis-Tsakonas, S., Matsuno, K. & Fortini, M.E. Notch signaling. *Science* **268**, 225–232 (1995).
27. Nye, J.S. & Kopan, R. Developmental signaling. Vertebrate ligands for Notch. *Curr. Biol.* **5**, 966-969 (1995).
28. Hunter, T. Oncoprotein networks. *Cell* **88**, 333–346 (1997).
29. Ellisen, L.W. *et al.* TAN-1, the human homolog of the Drosophila notch gene, is broken by chromosomal translocations in T lymphoblastic neoplasms. *Cell* **66**, 649–661 (1991).
30. Joutel, A. *et al.* Notch3 mutations in CADASIL, a hereditary adult-onset condition causing stroke and dementia. *Nature* **383**, 707–710 (1996).
31. Lindsell, C.E., Shawber, C.J., Boulter, J. & Weinmaster, G. Jagged: a mammalian ligand that activates Notch1. *Cell* **80**, 909–917 (1995).
32. Shawber, C.J., Boulter, J., Lindsell, C.E. & Weinmaster, G. Jagged2: A Serrate-like gene expressed during rat embryogenesis. *Dev. Biol.* **180**, 370–376 (1996).
33. Lindsell, C.E., Boulter, J., diSibio, G., Gossler, A. & Weinmaster, G. Expression patterns of Jagged, Delta1, Notch1, Notch2, and Notch3 genes identify ligand-receptor paires that may function in neural development. *Mol. Cell. Neurosci.* **8**, 14–27 (1996).
34. Bao, Z.Z. & Cepko, C.L. The expression and function of Notch pathway genes in the developing rat eye. *J. Neurosci.* **17**, 1425–1434 (1997).
35. Garrod, A. The lessons of rare maladies. *Lancet*, **1**, 1055–1066 (1928).
36. Elkahloun, A.G., Bittner, M., Hoskins, K., Gemmill, R. & Meltzer, P.S. Molecular cytogenetic characterization and physical mapping of 12q13-15 amplification in human cancers. *Genes. Chromosomes. Cancer* **17**, 205–214 (1996).
37. Beaudet, A.L. & Tsui, L.-C. A suggested nomenclature for designating mutations. *Hum. Mutat.* **2**, 245–248 (1993).